HYDROLOGICAL PROCESSES, VOL. 9, 383–400 (1995)

A PROCESS-BASED MODEL FOR COLLUVIAL SOIL DEPTH AND SHALLOW LANDSLIDING USING DIGITAL ELEVATION DATA

WILLIAM E. DIETRICH AND ROBERT REISS

Department of Geology and Geophysics, University of California, Berkeley, CA 94720, USA

MEI-LING HSU

Department of Geography, Univesity of California, Berkeley, CA 94720, USA

AND

DAVID. R. MONTGOMERY

Department of Geological Sciences, University of Washington, WA 98195, USA

ABSTRACT

A model is proposed for predicting the spatial variation in colluvial soil depth, the results of which are used in a separate model to examine the effects of root strength and vertically varying saturated conductivity on slope stability. The soil depth model solves for the mass balance between soil production from underlying bedrock and the divergence of diffusive soil transport. This model is applied using high-resolution digital elevation data of a well-studied site in northern California and the evolving soil depth is solved using a finite difference model under varying initial conditions. The field data support an exponential decline of soil production with increasing soil depth and a diffusivity of about 50 cm^2/yr. The predicted pattern of thick and thin colluvium corresponds well with field observations. Soil thickness on ridges rapidly obtain an equilibrium depth, which suggests that detailed field observations relating soil depth to local topographic curvature could further test this model. Bedrock emerges where the curvature causes divergent transport to exceed the soil production rate, hence the spatial pattern of bedrock outcrops places constraints on the production law.

The infinite slope stability model uses the predicted soil depth to estimate the effects of root cohesion and vertically varying saturated conductivity. Low cohesion soils overlying low conductivity bedrock are shown to be least stable. The model may be most useful in analyses of slope instability associated with vegetation changes from either land use or climate change, although practical applications may be limited by the need to assign values to several spatially varying parameters. Although both the soil depth and slope stability models offer local mechanistic predictions that can be applied to large areas, representation of the finest scale valleys in the digital terrain model significantly influences local model predictions. This argues for preserving fine-scale topographic detail and using relatively fine grid sizes even in analyses of large catchments.

KEY WORDS Process-based models Digital elevation data Slope instability Colluvial soil depths

INTRODUCTION

In steep, soil-mantled landscapes, shallow landsliding of the soil can generate debris flows which scour low-order channels, deposite large quantities of sediment in higher order channels and, in urbanized settings, destroy property and kill people (e.g. Costa and Wieczorek, 1987; Selby, 1993). The practical significance of shallow landsliding has motivated many different kinds of approaches to mapping the potential hazard in a watershed (see review in Montgomery and Dietrich, 1994). One approach that seems particularly promising is to use digital elevation data and simple coupled hydrological and slope stability models to delineate those areas most prone to instability (Okimura and Kawatani, 1987; Dietrich *et al.*, 1992; 1993; Wu, 1993; Montgomery and Dietrich, 1994).

0885-6087/95/030383-22
© 1995 by John Wiley & Sons, Ltd.

Received 30 March 1994
Accepted 23 October 1994

Soil thickness strongly affects relative slope stability, yet the spatial variation in soil thickness in landslide-prone areas is rarely estimated (two exceptions are Okimura, 1989; DeRose *et al.*, 1991; 1993). Soils are typically thin to absent on sharply defined ridges and thickest in unchannelled valleys. Vegetation provides a root strength to the soil, and on steep lands with organic-rich, low-density soils, this root strength may dominate or provide a significant portion of the total strength of the material. Vegetation can root through thin soils into the underlying bedrock typically found on ridges and side slopes and provide considerable strength. In thick soils typical of unchannelled valleys, slope instability is favoured because failure planes can form below the rooting depth and the topography forces subsurface flow convergence and elevated pore pressures (e.g. Dietrich and Dunne, 1978; Reneau, 1988; Crozier *et al.*, 1990).

Land-use and climate change modify vegetation. The local soil depth must be known to understand the influence of changes in vegetation on slope stability, yet such information is rarely available and it is impractical to measure for even a modest sized watershed.

Furthermore, soil thickness affects the availability of soil moisure, the relative role of subsurface to overland flow (e.g. Dunne, 1978) and, therefore, the general hydrological response of a landscape. It introduces a spatially organized influence on runoff processes through its dependence on topography, yet a lack of detailed field information inhibits incorporating these effects in models. In addition, by breaking down bedrock into smaller erodible sized particles, soil generation strongly influences the rate of landscape evolution (e.g. Kirkby, 1985; Anderson and Humphrey, 1989). On a practical level, land management decisions are ultimately made on the local level and it would be desirable to account for the local influence of soil thickness on slope stability. Hence there would be considerable value (for these and other problems) in a model that predicts the general spatial distribution of soil depth across a landscape.

Two kinds of models have been proposed to predict the spatial pattern of soil characteristics. Process-based models are few and only one appears to have attempted to relate a theoretical prediction with field observations. Ahnert (1970) described the results of a computer simulation which solves for the local 'waste cover' thickness as a mass balance between waste production and slope-dependent transport removal. He estimated waste cover thickness variation along several hillslope profiles in North Carolina and found that he could explain with his model the variation in cover thickness with local slope and distance from the divide. The most thorough model is that proposed by Kirkby (1985). He developed a model for the evolution of regolith-mantle slopes that determines the spatial distribution of a 'soil deficit', or the amount of original parent material remaining on a hillslope, as influenced by rock type and climate. This model, although instructive about the influence of weathering on slope evolution, requires a large amount of hydrological, mechanical and geochemical information to be applied to a specific site. Kirkby also only considered the developed of a soil along a hillslope profile.

Numerous empirical models for estimating the spatial variation in soil attributes have been proposed, and Moore *et al.* (1993) offer an excellent brief review of these studies. Moore *et al.* (1993) and Gessler *et al.* (in press) also propose a new method using correlations between observed properties and analysis of digital terrain. Such an approach enables high spatial resolution and estimation of many soil attributes other than depth, but requires a large amount of field data. Also, because of its empirical nature it can only apply to areas where it has been developed. Such models, although very useful, have only limited value in providing a mechanistic explanation for the spatial distribution of soil thickness.

Here we present a simple model for predicting the spatial variation in colluvial soil thickness and then use this model in a coupled hydrological and slope stability model to examine the influence of root strength on the pattern of slope instability. Our soil thickness model is similar to that described by Ahnert (1970), but it is developed in such a way that the parameters can be estimated from field observations and it is applied to a real three-dimensional landscape rather than a hillslope profile. Where the topography is reasonably well capature in the digital elevation data, our model successfully predicts the extent of thick colluvial deposits in unchannelled valleys and identifies areas of significant bedrock outcrop. The model also suggests that soil depth quickly tends to a constant value on divergent slopes, leading to a testable hypothesis about the relationship between topographic curvature and soil depth. Modelled slope stability is strongly influenced by the root cohesion, with slope instability most likely in the steep unchannelled valleys with thick colluvial deposits, a result in agreement with field observations. In contrast with river systems which can drain very large areas, hillslopes are of finite extent, hence it is possible to apply the soil depth and slope stability models to local areas in large watersheds using fine scale grids.

THEORY FOR COLLUVIAL SOIL THICKNESS

Here we briefly describe a model for soil depth and show examples of its application to a site where we have mapped the pattern of thick colluvium and located shallow landslide scars. A more detailed development of the soil model can be found elsewhere (Dietrich *et al.* in prep.). The term 'soil' is used here to mean the surficial material mantling the underlying weathered or fresh bedrock and lacking relict rock structure. In thin soils it is roughly equivalent to the solum (the A and B horizons) and in areas of thick accumulations due to mass wasting it is equivalent to colluvium. As long as there is a gradient to the topography, however, all soils in this model are colluvial rather than residual.

This model is thought to be most applicable to unglaciated landscapes underlain by mechanically strong bedrock lacking a well-developed saprolite. We do not consider the role of chemical and physical breakdown of the underlying rock and its influence on soil generation in this model. Although such processes are certainly important, for simplicity we have chosen not to treat them explicitly in the model. Instead, we use a general soil production function proposed by others for which we have some field evidence. The soil production function we use may represent the role of biogenic processes in mechanically disrupting the underlying bedrock and converting it to a mobile soil layer. In the following we emphasize the role of such processes, but the general model does not specifically require only biogenic processes to occur.

On many hilly landscapes, the loose surface soil appears to be largely derived from the underlying bedrock by biogenic processes that dig into the bedrock and force pieces of it into the soil layer or onto the ground surface. In our experience in such landscapes, the transition from the soil to the underlying bedrock is usually abrupt. The most obvious example of this mixing of bedrock into the soil occurs by tree throw. We have observed in many environments, including in the Pacific Northwest, Puerto Rico and Australia, clear instances where the uplifted root wad of the fallen tree still contained bedrock with recognizable structures such as bedding. As the roots decay the bedrock will break into pieces, tumble to the ground and become part of the mobile soil layer. Other obvious agents of mixing of bedrock into the soil include the burrowing effects of animals and insects.

When these biogenic processes operate on an inclined surface, the presence of a downslope component of gravity presumably causes a net transport downslope at a rate roughly proportional to the gradient. Soil thickness is then the result of the dynamic balance between the downslope changes in the rate of transport and the production rate of soil (Figure 1). If solution processes play a minor part in mass transport, the conservation of mass equation for soil thickness, h, can be written as

$$\rho_s \frac{\partial h}{\partial t} = -\rho_r \frac{\partial e}{\partial t} - \nabla \cdot \rho_s \tilde{q}_s \qquad (1)$$

where ρ_s and ρ_r are the bulk density of soil and rock, respectively, e is the elevation of the bedrock–soil interface and $\tilde{q}_s$ is the soil transport vector. The first term is the change in soil thickness with time, t. The second term is the rate of conversion of bedrock to soil due to lowering of the bedrock–soil interface and the last term is the divergence of soil transport.

To solve Equation (1) for the spatial variation in soil depth, we need a transport law for q_s and a soil production law. The simplest approach is to consider the case where hillslope processes can be represented by a purely slope-dependent transport law

$$\tilde{q}_s = -K \nabla z \qquad (2)$$

in which K is a parameter equivalent to a diffusion coefficient with units of L^2/t and is assumed to be isotropic. Such a law has its origins in the works by Davis (1892) and Gilbert (1909), has been used in analytical and numerical models of landscape evolution (i.e. Culling, 1963; Kirkby, 1971; Koons, 1989; Anderson and Humphrey, 1989; Howard, 1994; see review in Fernandes and Dietrich, in prep.), and has some field evidence to support the simple linear dependence on gradient (McKean *et al.*, 1993). The

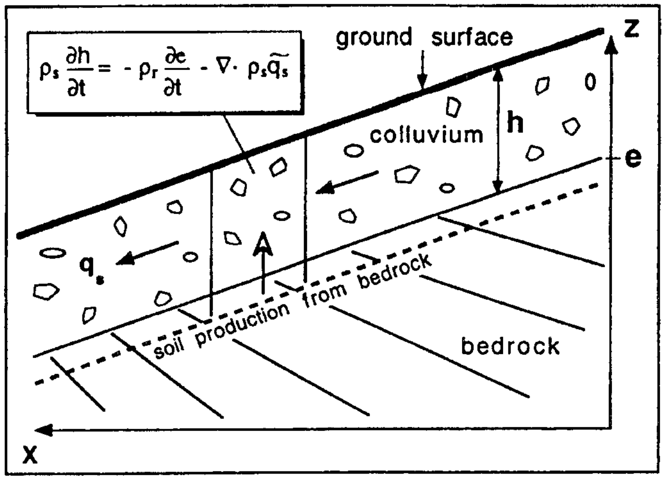

Figure 1. Balance of soil transport and production which controls local colluvial soil depth. In our study area, mass transport downslope, q_s, of the entire active layer of the soil is caused primarily by biogenic processes acting on an inclined surface. The equation in the figure is Equation (1) in the text and all terms are defined there and shown graphically in the figure. The shaded area between the base of the soil at elevation e and the broken line is the amount of bedrock that would be converted to soil over some specified time interval. Note that $z = e + h$

diffusion coefficient in Equation (2) is not an arbitrary constant, but rather can be estimated by a variety of field methods, but when used in modelling its value is clearly scale-dependent, increasing in magnitude from hillslopes to mountain ranges (see review in Fernandes and Dietrich, in prep.). Equation (2) does not apply to runoff-driven transport responsible for valley evolution, nor is it apparently applicable to landsliding. It could be argued that the gradient term should be given by the sine of the slope (A. Howard, pers. comm.), but we will not consider that effect here.

The approach we will take is to apply Equation (2) to real landscapes represented by a digital elevation field in which diffusive transport processes predominate on the ridges and tend to fill the valleys between short periods of erosion by landsliding and gullying. In our experience such landscape processes typify (but are not limited to) unglaciated, hilly, mostly soil-mantled landscapes in humid to semi-arid climates where Horton overland flow is rare or absent and the underlying bedrock is mechanically strong. By ignoring the effects of river incision at the base of slopes and landsliding, we are in effect taking the digital landscape as given and solving for what the soil distribution should tend to be for the present topography under the assumption that landform change is sufficiently slow that soil depth tends to the local steady-state condition (of either constant depth or constant aggradation). The relatively narrow range of soil depth on hillslopes and the systematic thickening of soil in unchannelled valleys in our field sites support this assumption.

Despite its importance, we known of no field study that defines the production law for an area. Cox (1980) summarizes various theoretical expressions for this law, all of which are based on the assumption that the production rate is a function of the thickness of the soil. Since the original suggestion by Gilbert (1877) it has been assumed that the production rate is zero for soils greater than some depth and that for shallow soils the production rate increases, perhaps reaching a maximum when the bedrock is exposed or at some intermediate soil depth (Figure 2). It was the inference that the production rate reaches some maximum that led (thanks in large measure to Carson and Kirkby, 1972) to the now widely used terms, transport-limited (where there is a soil mantle) and weathering-limited (bedrock at the surface) landscapes. Ahnert (e.g. 1988) has offered the most specific relationships between weathering rate and 'cover thickness', reasoning that mechanical weathering decreases exponentially with cover thickness, but chemical weathering increases with increasing thickness, leading to a weathering rate that has a maximum at some finite cover thickness. An argument can be made that if mechanical disruption by biota plays a major

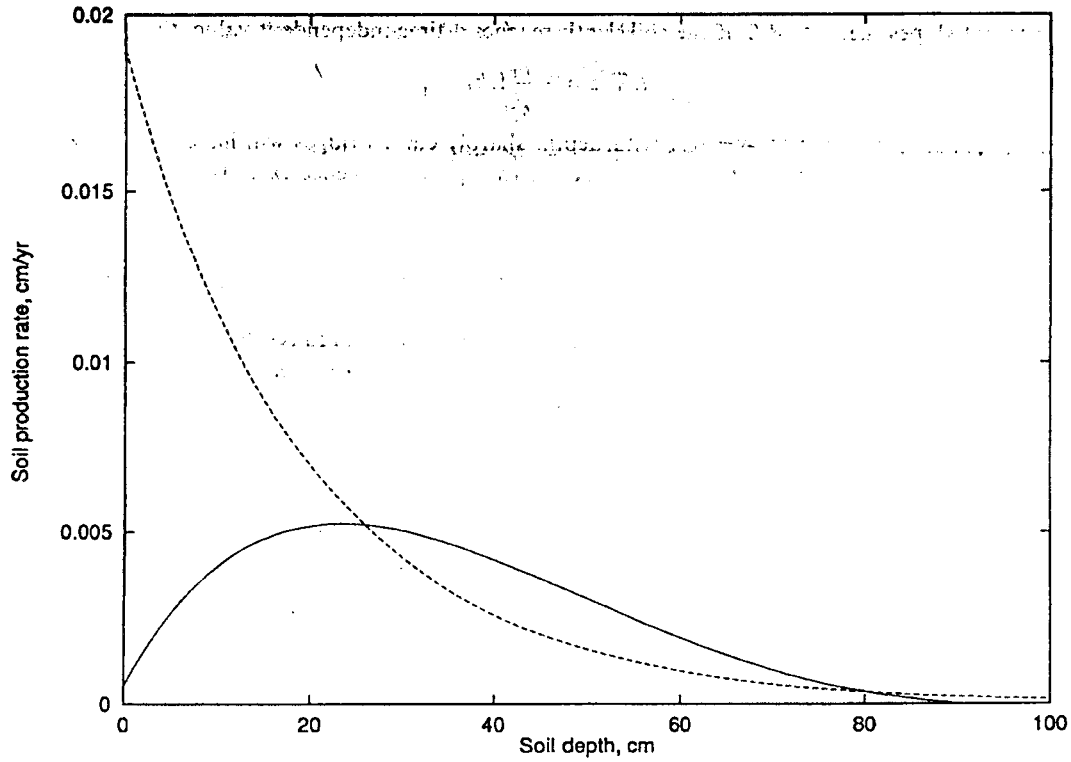

Figure 2. Two production functions estimated from field data. The exponential function was fitted to two data points: 0·0042 cm/yr at 30 cm and 0 at 150 cm. The other function, represented by a polynomial which gives a peak at about 25 cm, was set to a peak close to the 30 cm value for the exponential, but the intercept value is arbitrarily low and the production was assumed to go to zero at 90 cm. Note that the production rate is $-\partial e/\partial t$ and that at equilibrium on the ridges this rate is equal to $-K(\rho_s/\rho_r)\nabla^2 z$

part in converting in place bedrock to mobile soil, a similar 'humped' production curve may be appropriate. The frequency of contact and disruption of the colluvium–bedrock boundary should decrease as the soil thickens, hence production should tend to decrease with thickening soil. It is reasonable to suspect that sufficiently thin soil cannot support burrowing animals and that completely exposed bedrock has a lower rate of conversion to soil than that which is partly buried.

We have explored two general kinds of production laws, one which is a simple exponential decline with thickening soil, i.e. $-\partial e/\partial t = P_0 e^{-mh}$ (in which P_0 and m are empirical constants) and one in which the soil depth is a complex, bell-shaped function of h, with a maximum at some thin soil value (Figure 2). So, in general (assuming K and ρ_s are spatially constant), we can write for $f(h) = -(\partial e/\partial t)$

$$K\nabla^2 z = \frac{\partial h}{\partial t} - \frac{\rho_r}{\rho_s} f(h) \tag{3}$$

If the production rate reaches zero with increasing thickness, then valleys which receive convergent sediment transport will tend to fill and the local production rate will reach zero, leading to

$$K\nabla^2 z = \frac{\partial h}{\partial t} \tag{4}$$

The deposition rate in valleys is set by the diffusion coefficient and the topographic divergence; the total amount of soil deposited depends on how long aggradation has occurred since the last evacuation event (see Reneau, 1988; Reneau *et al.*, 1989; 1990). This result is most applicable to unchannelled valleys.

On divergent slopes, i.e. $\nabla^2 z < 0$, if the soil depth reaches a time-independent value, then

$$K\nabla^2 z = -\frac{\rho_r}{\rho_s} f(h) \tag{5}$$

and if the production rate varies inversely with depth, sharply curved ridges will have the thinnest soils. Bedrock will appear at the surface, however, where the transport divergence exceeds the production rate

$$-K\nabla^2 z > \frac{\rho_r}{\rho_s} f(h) \tag{6}$$

Anderson and Humphrey (1989) point out this effect in a more complicated one-dimensional model which includes landsliding.

Once bedrock appears, the proposed transport law no longer applies because there is insufficient soil to satisfy the net soil flux. In our finite difference numerical model, for those elements where the transport rate from the element exceeds the sum of the soil thickness, the production amount and the upslope influx of soil, we reduce the transport rate to the total available from these three sources.

THEORY FOR THE INFLUENCE OF SOIL DEPTH ON SHALLOW SLOPE INSTABILITY

In earlier papers we have proposed simple theories for coupled shallow subsurface flow and landsliding of the soil mantle (i.e. Dietrich *et al.*, 1986; 1992; 1993) which did not explicitly account for the influence of soil depth, unlike the innovative model proposed by Okimura and Kawatani (1987). Our previous model uses a steady-state runoff model to define the topographic control on pore pressure distribution and the resultant spatial pattern of slope instability. Soil cohesion is not included and the angle of internal friction and soil bulk density have been treated as spatially constant. We have shown that this very simple, one to two parameter model fairly accurately delineates those parts of the landscape prone to shallow landsliding (Dietrich *et al.*, 1993; Montgomery and Dietrich, 1994). The model, however, does not account for the effects of vegetation change on slope instability and therefore cannot explicitly examine the effects on vegetation and slope stability. Also the model uses the assumption that the saturated conductivity is invariant with depth which is far from the case in natural landscapes. Here we take advantage of our soil model to estimate the effect of exponentially declining saturated conductivity and varying cohesive strength due to roots on the pattern of slope instability. An important question we will address is whether this much more complicated model offers substantial improvements in estimating the location of shallow landsliding.

We use the infinite slope model (e.g. Selby, 1993) which accounts for the strength contributed by roots as an apparent cohesion, C_r,

$$\rho_s g h \sin\theta\cos\theta = C_r + C_{sw} + (\rho_s g h \cos^2\theta - \rho_w g u \cos^2\theta)\tan\phi \tag{7}$$

in which g is gravity, θ is the hillslope angle, C_{sw} is the cohesion of the soil when it is wet, ρ_w is the density of water, ρ_s is the soil bulk density (including the mass contribution from soil moisture), u is the pore pressure and ϕ is the angle of internal friction. The vertical surcharge of vegetation is neglected and short-term changes in root strength due to land use are not considered here (see Sidle, 1992). This slope stability equation is linked to the hillslope hydrology through the pore pressure term in which

$$u = h - y_w \tag{8}$$

and y_w is the distance below the surface to the water-table. As such Equation (8) only applies if $y_w \leqslant h$. When the water-table is below the bedrock–soil interface, then u is assumed to be zero. The wet soil bulk density varies from saturated values to moist values, but for simplicity we just use the saturated values. If Equation (8) is substituted into Equation (7) for the pore pressure term, then the equation can be solved for the ratio of the distance below the surface to the water-table, y_w and the soil depth, h

$$\frac{y_w}{h} = 1 - \frac{\rho_s}{\rho_w}\left[1 - \frac{1}{\tan\phi}\left(\tan\theta - \frac{C_r + C_{sw}}{h\rho_s g\cos^2\theta}\right)\right] \tag{9}$$

Failure will occur even when the water-table is below the bedrock interface when

$$\tan\theta \geqslant \frac{C_r + C_{sw}}{h\rho_s g\cos^2\theta} + \tan\phi \tag{10}$$

and land this steep is unconditionally unstable. Slopes with sufficiently low gradient that they will not fail even when saturated, occurs if

$$\tan\theta \leqslant \frac{C_r + C_{sw}}{h\rho_s g\cos^2\theta} + \tan\phi\left(1 - \frac{\rho_s}{\rho_w}\right) \tag{11}$$

Field evidence suggests that saturated conductivity declines exponentially through the soil and through the underlying bedrock, but at different rates (Montgomery, 1991), such that we can write

$$k = k_1 e^{-n_1 y\cos\theta} \qquad \text{for } y \leqslant h \tag{12}$$

and

$$k = k_2 e^{-n_2 y\cos\theta} \qquad \text{for } y > h \tag{13}$$

where k is the saturated conductivity (assumed to be isotropic) at vertical distance y below the surface and k_1 is the saturated conductivity at the ground surface and k_2 is this value when the bedrock values are projected to the ground surface. The exponents for these equations (n_1 and n_2) account for the decrease in saturated conductivity normal to the ground surface rather than vertically, and that is why the $\cos\theta$ is included. Following the approach used previously (Dietrich *et al.*, 1992; 1993, Montgomery and Dietrich, 1994), we solve for the steady-state runoff by subsurface flow parallel to the ground surface (hence given by the topographic gradient, $\sin\theta$), by integrating Equations (12) and (13) and multiplying by the assumed head gradient

$$qa = \left[\int_{y_w}^{y=h_0} k_1 e^{-n_1 y\cos\theta}\partial y\cos\theta + \int_{y=h_0}^{\infty} k_2 e^{-n_2 y\cos\theta}\partial y\cos\theta\right] b\sin\theta \tag{14}$$

in which q is the precipitation minus evapotranspiration which falls on the horizontal surface area, a, and flows across the unit contour length, b. The depth, h_0, is equal to the soil depth, h, unless the change in slope (from n_1 to n_2) occurs within the colluvium, which can happen in thick unchannelled valley-fills (Montgomery, 1991). In this latter case, h_0, is equal to h up to the depth where it changes and then it is fixed at that depth value.

Integrating Equation (14) and solving for y_w/h, gives

$$\frac{y_w}{h} = \frac{1}{-n_1 h\cos\theta}\ln\left(\frac{qan_1}{k_1 b\sin\theta} + e^{-n_1 h_0\cos\theta} - \frac{k_2 n_1}{n_2 k_1}e^{-n_2 h_0\cos\theta}\right) \tag{15}$$

A single equation coupling the slope stability and the hydrological model can then be obtained by setting Equations (15) and (9) equal, and solving for the ratio of effective rainfall rate to the saturated conductivity at the surface

$$\frac{q}{k_1} = \frac{b\sin\theta}{an_1}\left(e^{-n_1\beta h\cos\theta} - e^{-n_1 h_0\cos\theta} + \frac{k_2 n_1}{n_2 k_1}e^{-n_2 h_0\cos\theta}\right) \tag{16}$$

where

$$\beta = 1 - \frac{\rho_s}{\rho_w}\left[1 - \frac{1}{\tan\phi}\left(\tan\theta - \frac{C_r + C_{sw}}{h\rho_s g\cos^2\theta}\right)\right] \tag{17}$$

In this dimensionless form Equation (16) can easily be used in a digital terrain model in which topographic attributes, θ, a and b, can be measured and the differing values of the ratio of effective rainfall to infiltration rate needed for instability can be mapped. The local soil depth, h, is estimated from numerically solving Equation (3). Nine parameters must be specified to use Equation (16) once the topographic and soil depth field has been defined: h_0, n_1, n_2, k_2, k_1, $\tan\phi$, ρ_s, C_s and C_r. An argument can be made that these parameters should not be single valued, but should be assigned probability distributions (e.g. review in Mulder, 1991). Because field observations suggest that these parameters probably vary in space systematically rather than randomly (co-varying, for example, with soil depth), this would require assigning this spatial correlation structure, further complicating the model. For simplicity here we treat these parameters as spatially constant.

For a given landscape the strength properties contained in β determine the range of slopes susceptible to instability. The topographic term, $b \sin\theta/a$, in Equation (16) shows that for this steady-state model, lower gradient (but steep enough to fail), strongly convergent (low b/a) areas are least stable. The lower gradient is favoured because destabilizing pore pressures build up with less rainfall on lower gradient hillslopes. Intense precipitation much shorter in duration than that necessary for a steady-state response may favour instead steep side slopes as the least stable (Hsu and Dietrich, in prep.).

Equation (16) also shows that the amount of precipitation necessary for instability varies directly with the saturated conductivity at the ground surface, k_1, and inversely with the rate of decline of the conductivity in the soil, n_1. As in all subsurface flow problems, a meaningful saturated conductivity is difficult to define from field data, but has a large effect on the result. Because we have used k_1 to normalize our results, and because it appears as part of a ratio in the third term on the right-hand side, we do not need to know the exact value of k_1 unless we wish to judge the model in terms of whether it requires reasonable amounts of precipitation. Given that the model is steady state, which rarely, if ever, occurs in most natural storms, evaluating the precipitation rate required for instability may not be instructive: the primary result is the relative rating given by Equation (16) in its dimensionless form. Hence small q/k_1 means least stable and large q/k_1 is most stable. One reason, however, to attempt to assign specific values to the hydrological parameters, k_1, k_2, n_1, n_2, is to estimate whether the rainfall associated with a large q/k is so great as to indicate that the chances of instability are very low. This has obvious practical implications. We explore this problem in the application section.

Soil depth must be prescribed to estimate the role of cohesion in contributing strength to the soil; the deeper the soil the less significant the contribution from cohesion. The strong tendency for soils to be thin on narrow ridges and thick in convergent areas enhances the importance of steep unchannelled valleys as debris flow source areas (see review in Reneau and Dietrich, 1987b). Not only are unchannelled valleys typically mantled with a thicker colluvium which reduces the effectivness of root cohesion, but they are less stable because of the hydrological effects of topographic convergence (Dietrich *et al.*, 1986). Because of the thicker colluvium in unchannelled valleys these features, when they fail, produce larger, more destructive debris flows. Hence the coupled soil depth–slope stability model may be particularly useful in identifying debris flow hazards.

A test of the usefulness of Equation (16) is to apply it with and without a spatially varying soil depth to determine if, when applied to a real landscape, the range in depth and its spatial distribution has a primary influence on the location of shallow landsliding. If the topography dominates the location of shallow landsliding, then even a simpler model which we have previously used (Dietrich *et al.*, 1992; 1993; Montgomery and Dietrich, 1994) may be sufficient. This simpler model has the advantage of having only two parameters.

APPLICATION OF MODELS

In using Equations (3) and (16) in a digital terrain model, the first consideration should be whether the hydrological and erosion processes represented by these models actually occur in the landscape of interest. The soil depth model in the form given in Equation (3) assumes that over the time period sufficient to influence soil depth, the dominant hillslope transport process can be represented by a slope-dependent transport law. The slope stability model assumes that shallow subsurface flow parallel to the ground surface dictates the build-up of pore pressures and that instability involves just the weaker colluvial mantle. Also important is the quality of the digital elevation data. If the grid cells are large and therefore unable to portray either the local slope or the unchannelled valleys accurately, application of Equations (3) and (16) would seem unwarranted, and a simpler model such as that described in Montgomery and Dietrich (1994) would be more appropriate.

We use a grid-based rather than a contour-based model because it is substantially easier to apply these models and evolve the land surface over large basins. To reduce the grid artifacts, drainage area, slope and transport are determined in all eight possible directions. Programs available in ARC/INFO were used to grid the original data and to generate figures. Details of our finite difference numerical model are given elsewhere (Dietrich *et al.*, in prep.).

Field site

We apply these models to a small watershed in Tennessee Valley, Marin County, California, where we have approximately 10 m resolution digital elevation data, extensive field observations about runoff and erosion processes, and where we have already tested the simpler, depth-independent slope stability model (Montgomery and Dietrich, 1989; Montgomery, 1991; Dietrich *et al.*, 1992; 1993; Montgomery and Dietrich, 1994). The area is mostly underlain by tectonically deformed greywacke with some greenstone and chert. Colluvial soils mantle the landscape with thick deposits (several metres) in unchannelled valleys and thin soils on the ridges giving way to bedrock outcrops. Bedrock also crops out on steep side slopes and canyon bottoms. Grass and chaparral predominate in these hilly lands. There is clear evidence of biogenic processes playing a major part in mobilizing fractured bedrock into the shallow soil mantle and in causing the downslope transport of debris. Debris slide scars involving just the soil mantle are common. In the following we parameterize the model based on field observations and test the utility in explaining observed phenomena.

Soil depth

To apply Equation (3) to Tennessee Valley, we need an estimate of the diffusivity, K, the bedrock and soil density, and the production function. Reneau (1988) estimated diffusivity by solving Equation (2) for K by dividing a calculated flux of sediment required to in-fill unchannelled valleys (based on radiocarbon determined deposition rates) by the mean gradient of the adjacent source slopes. This gives a roughly Holocene averaged diffusivity. As reported in McKean *et al.* (1993), data supplied by Reneau (1988) for 34 unchannelled valleys in the coastal mountains of California, Oregon and Washington gave a mean diffusivity of $49 \pm 37\,cm^2/yr$, with no clear regional differences. The nearest and most similar sites to Tennessee Valley gave values of 54 and $44\,cm^2/yr$. Here we will use $50\,cm^2/yr$. The bedrock to soil density ratio is, according to data in Reneau (1988) about 1.7.

The production function is not known, but we have some guidance from field data of what might be reasonable. Bulk density profiles in the thick colluvial deposits of the unchannelled valleys of this area show a near-linear decrease with depth to about 1.5 m and then remain nearly constant (Reneau, 1988). These deposits accumulate from convergence transport caused by the diffusive-like effects of frequent biological disturbance, largely due to burrowing mammals in this area (e.g. Black and Montgomery, 1991). The depth profile may reflect the decrease in dilational effects of biogenic mixing (see Brimhall *et al.*, 1992), for discussion of this phenomenon), with penetration very rare below 1–1.5 m. Field observations of depth of rooting and animal burrows are congruent with this interpretation. Hence we suggest that the production of loose soil from the underlying weathered bedrock stops once a soil reaches this depth. At the two nearby sites where the diffusivity was determined, the average soil depth on the convex side slopes which serve as sources for the sediment that accumulates in the valleys is about 30 cm. Assuming the soil depth to remain constant during the period of accumulation in the valley axis we can estimate the bedrock to soil conversion rate from the net erosion recorded in the thickened deposits in the valley axis. For the two sites this value is 0.035 and 0.05 mm/yr. Here we assume that soil is produced at the rate of 0.0042 cm/yr from bedrock for a 30 cm thick layer of soil. By fitting an exponential function, $-\partial e/\partial t = P_0 e^{-mh}$, to the thick (no production at 150 cm) and thin soil production rates (0.0042 cm/yr at 30 cm) we obtain $P_0 = 0.019$ cm/yr and $m = 0.05$ (for a soil depth in cm). For depths greater than 100 cm, the productivity rate is assumed to be zero.

We could reason that maximum production should occur at some intermediate depth most favourable to biological activity and frequent contact with the underlying bedrock. In our study area, pocket gophers are common, and generate tunnels about 5 cm in diameter. As an alternative to the exponential function, we

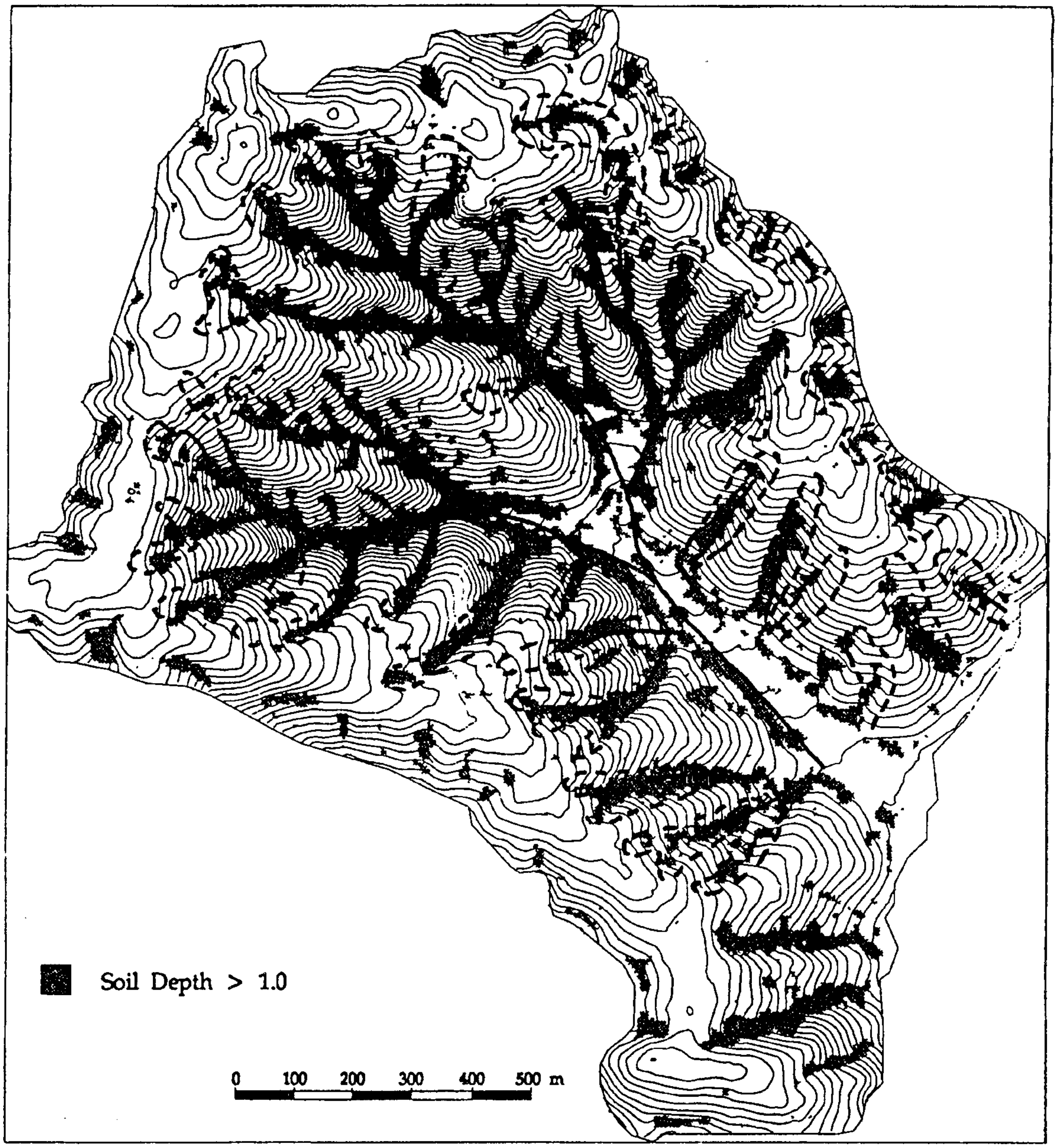

Figure 4. Comparison of predicted pattern of soil depth with areas of thick colluvium mapped reported by Montgomery and Dietrich (1989) on a different topographic base map. Shaded area are elements in Figure 3 with depth greater than 1 m. Channel network mapped in the field is shown as a solid line; some tributary channels do not connect to the main branch. Mapped boundaries of thick colluvium are shown with broken lines that mostly define nearly closed loops at the end or surrounding first-order channels

have selected a peak production at 25 cm (Figure 2). Given the lack of data to specify this function, we have made the peak production close to the observed value (at 30 cm depth) and assigned an arbitrarily low value at the zero depth intercept.

Numerical experiments show that the model is insensitive to the initial soil depth, so we selected 30 cm as a value close to that for much of the ridges. Radiocarbon dating of basal colluvium in this area indicates that deposition began at about 9000 to 15 000 years ago (Reneau *et al.*, 1990), hence a run time of 15 000 years was chosen to generate the soil depth. We found that the model gave consistent results if we used 100 year time steps or less. Hundreds of numerical experiments have been performed, but with limited space here we give only two examples.

Figure 3 shows the predicted pattern of soil depth after 15 000 years for a 5 m grid spacing for the exponential case. No tuning of any of the parameters has been performed. As observed in the field, narrow ridges have the thinnest soils and thick colluvium has accumulated in the valleys. This might be the pattern of soil depth if all incision due to water runoff ceased. Such processes present soil build-up in the larger valley bottoms and locally roughen the topography. We have not accounted for this effect. Figure 4 shows the mapped pattern of thick colluvium reported by Montgomery and Dietrich (1989) using a completely different and coarser base map before the digital elevation data were available. There is good correspondence between the mapped and predicted area of thick (greater than 1.0 m) colluvium. Also shown is the mapped channel network which, where it extends downslope of the colluvial valleys, is bedrock or alluvial-mantled. The edges of the area shown which lack the heavy lines were not mapped in 1989. In the centre of the map area, however, several small valleys are predicted to have thick colluvial deposits, but instead are mostly thinly mantled bedrock. This appears to be due to scour by shallow landsliding.

The alternative production law, with the peak production at 25 cm, gives substantially different results (Figure 5). The lower peak value causes many of the more sharply curved ridges to have bedrock at the surface — a result inconsistent with field observations. This effect could, of course, be eliminated if we put the peak up as high as the exponential intercept with zero depth, but this will not eliminate one other inconsistency. As explained by Carson and Kirkby (1972) for a similar production function, soil depths on the left-hand side of the peak of the production rate are not stable values. Without erosion, soil will simply progressively thicken to the point where production declines to zero. With soil erosion, thinning of the soil will decrease to induce less soil production, and this will lead to stripping of the soil to bedrock. Hence there should be no equilibrium soil depth values observed in the field less than the depth of peak production if the 'humped' production law is to apply. In our study site, soil depths between zero to 25 cm are common on ridges. Our modelling suggests that depth adjustments are rapid on thin soils, hence these thin soils are probably in local equilibrium (erosion approximately equals production). Therefore, if a peak production exists, it must occur at soil depths close to zero, rather than at a depth of 25 cm as chosen.

For this landscape the exponential function is the simplest and is determined empirically. We do not yet know when once the bedrock completely emerges at the surface whether the prodcution rate actually drops or stays at the high value given by the exponential projection to zero depth. For the problems examined here, this distinction is not essential.

In Figure 6, the rate of surface elevation change ($\partial z/\partial t = \partial h/\partial t + \partial e/\partial t$) is plotted against the divergence of sediment transport ($K\nabla^2 Z$) for each cell used to create Figure 3 (soil depth after 15 000 years). The data fall along two distinct relationships. In convergent areas (valleys), net deposition halts soil production ($\partial e/\partial t = 0$) once the depth exceeds 1 m. Equation (4) then applies, giving the linear relationship shown in Figure 6, with a slope of 1.0. In divergent areas (ridges), a balance developes between the production rate and the divergence of sediment transport, soil thickness is time dependent ($\partial h/\partial t = 0$) and Equation (5) then applies. The slope of this linear relationship, then, is ρ_r/ρ_s, the rock to soil bulk density ratio. This general tendency for the landscape to be divided into hillslopes with time-independent soil thickness and valleys with a net accumulation is quickly established (within several thousand years). This suggests that unless a significant recent landslide or a climatically driven change in the production rate or diffusivity has occurred, the soil thickness on divergent areas should be at equilibrium thickness values.

The model smoothes the initial topography, most rapidly removing the sharp curves (as long as the bedrock does not emerge). If the model is run for a period much longer than that dictated by the age of the colluvial fills (more than 30 000 years at our site), the topographic contours become very smooth and much of the local depth variation is eliminated. Although initial gridding of the digital elevation data introduces some artificial roughness which is removed by diffusive transport, we elected to use the value

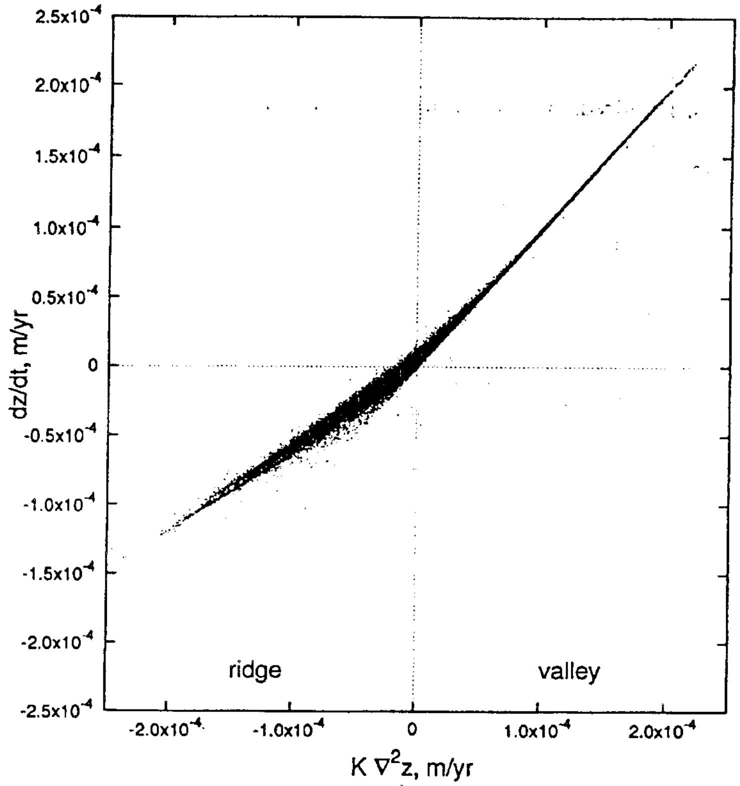

Figure 6. Plot of rate of vertical elevation change of the ground surface as a function of local topographic curvature, $\nabla^2 z$, times the diffusion coefficient after 15 000 years

of soil depth at 15 000 years with the initial topography to drive the slope stability model to retain as much of the present topographic influence on slope stability as possible.

Slope stability

To apply Equation (16), four strength parameters and five hydrological parameters must be estimated. Although the model would allow these parameters to be specified individually for each cell, unlike the soil depth model we have no theory or field evidence for the spatial structure of these parameters, so here we assign one value for the entire area. Based on sampling and testing reported elsewhere (Reneau and Dietrich, 1987a; 1987b; Dietrich *et al.*, 1993), we estimate ϕ to be 40°, the wet soil bulk density to be 2000 kg/m^3 and the soil cohesion to be zero. Root cohesion varies with vegetation type and we will examine the effect of varying cohesion on the predicted pattern of instability.

Values for the hydrological properties are estimated from falling head tests performed by D. Montgomery in Tennessee Valley area on piezometers in the thickened colluvium around a channel head (Montgomery and Dietrich, in press) and by C. Wilson in a nearby basin where tests were performed on shallow side slope colluvium, underlying bedrock and in deep colluvium and underlying bedrock in two hollows (Wilson and Dietrich, 1987; Wilson, 1988). Montgomery's data show the shallow colluvium in the hollow at his study site to have a saturated conductivity greater than 2×10^{-4} m/s and to decrease slowly with depth below the surface. Wilson's data suggest that the thinner side slope colluvium may be less conductive than in the hollow axis and that the bedrock immediately underneath the colluvium is about 10 times less conductive and declines with depth more rapidly. Wilson and Dietrich (1987) and

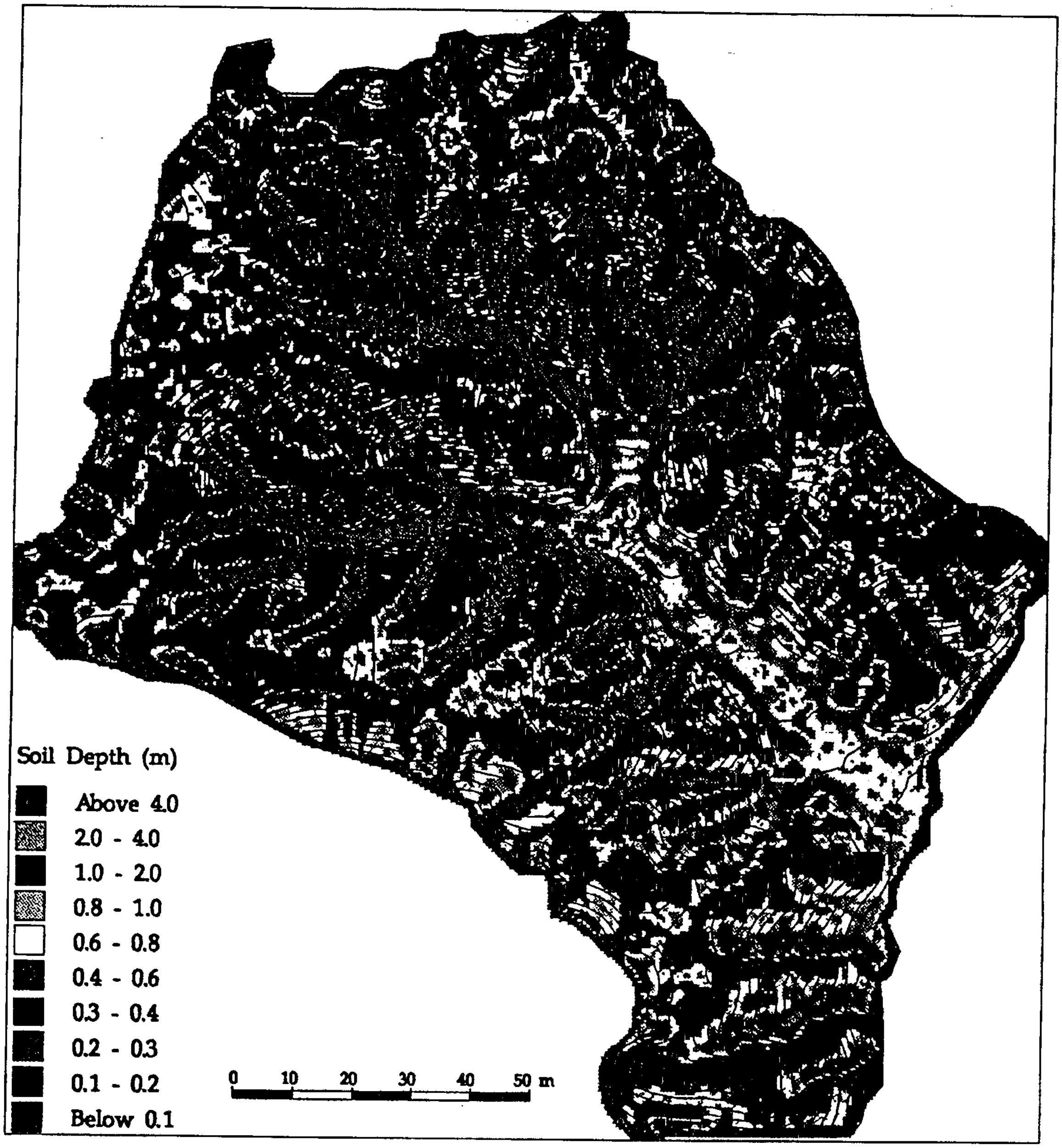

Figure 3. Predicted pattern of soil depth in Tennessee Valley after 15,000 years for K = 0.005 m^2/yr, initial soil depth of 0.3 m, bulk density ratio of rock to soil of 1.7 and the exponential production function, i.e.$-\partial e/\partial t = 0.019$ cm/yr $e^{-0.05 * \text{soil depth}}$. Calculations were performed in 100 year time steps for 5 m elements. Legend gives the soil depth categories in metres

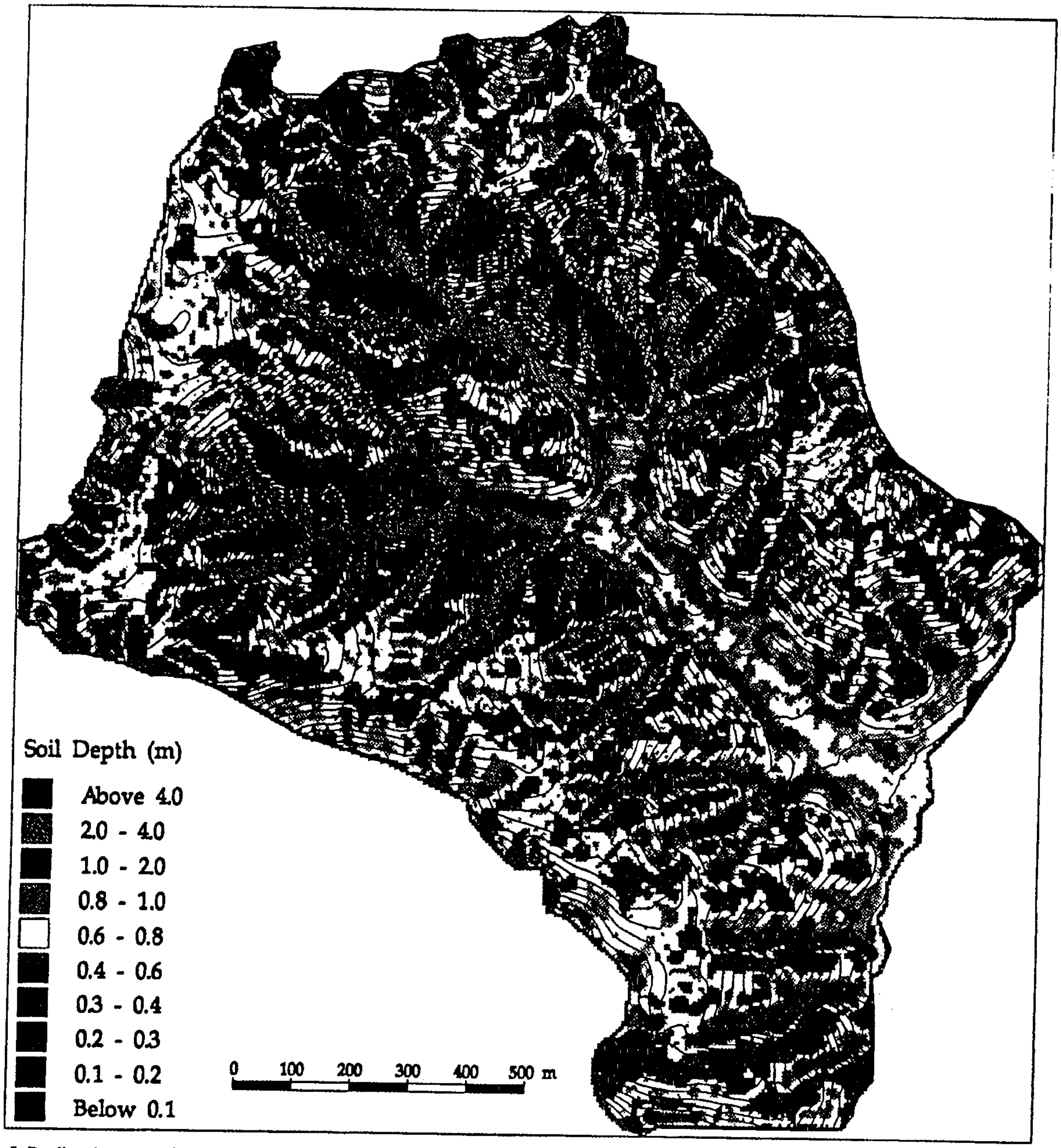

Figure 5. Predicted pattern of soil depth in Tennessee Valley after 15,000 years using the same parameters as in Figure 3, except the production function has a peak at 25 cm, as shown in Figure 2

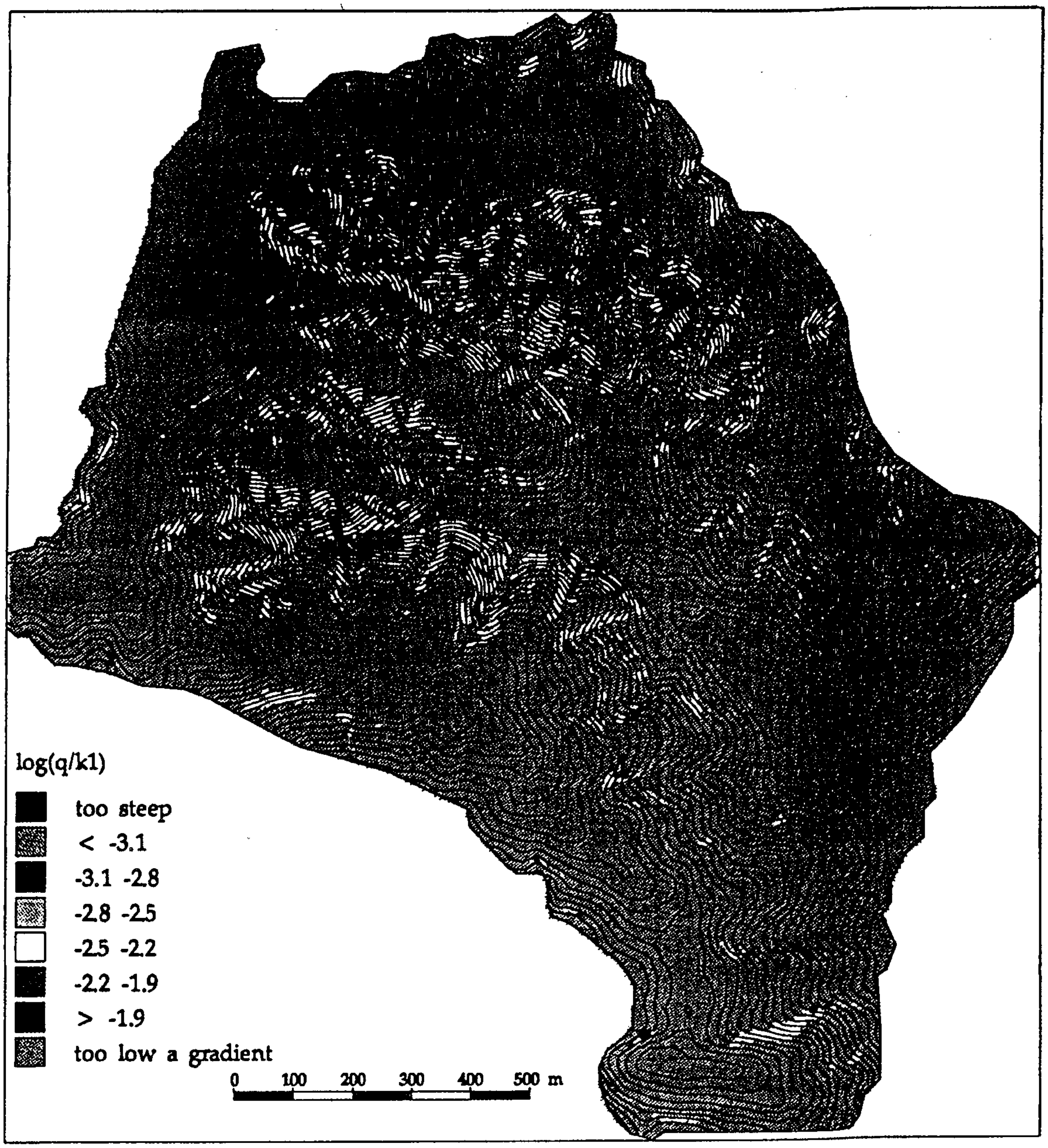

Figure 7. Predicted and observed pattern of slope instability in Tennessee Valley using Equation (16) in text. Soil depth is that shown in Figure 3. Angle of internal friction is 40°, root cohesion is 1000 N/m², $n_1 = 0.5$, $n_2 + 1.4$, $k_2/k_1 = 0.2$. Relative stability is shown by the logarithm of the ratio of effective precipitation to surface infiltration rate, with high negative values implying the small amounts of steady-rate rainfall necessary for instability. The black outlines are the approximate location of the debris slide scars. The scars are shown larger than their actual size to account for plotting uncertainty with regard to location

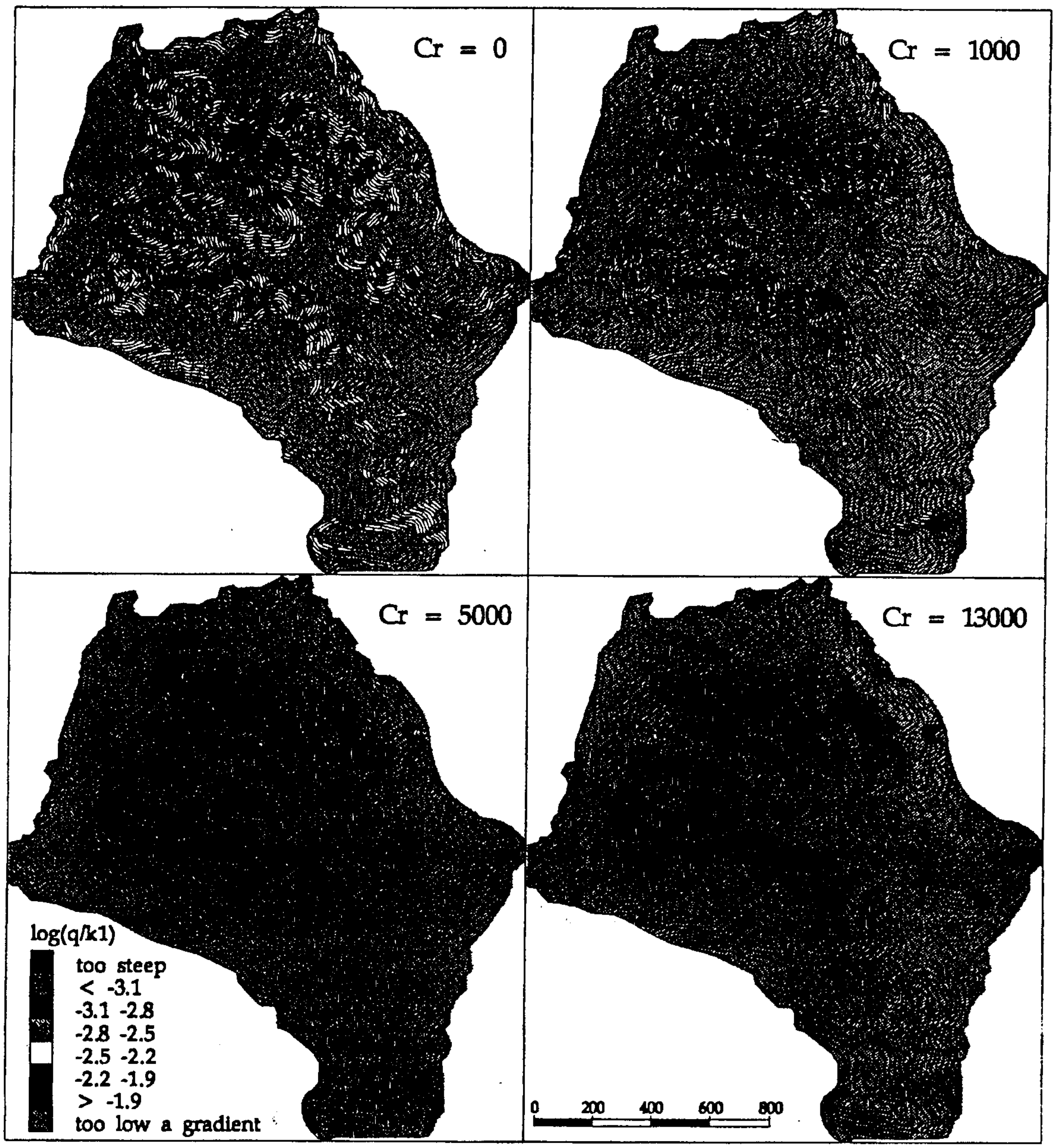

Figure 8. Comparison of the relative slope stability with changing root strength, C_r, shown in N/m². All other factors the same as in Figure 7 and this figure is repeated here without the landslide scars

Wilson *et al.* (1989) demonstrate that although the bedrock is less conductive it contributes to storm flow in large rainfall events. Our best estimate, which combines these two data sets, is $k_1 = 2 \times 10^{-4}$ m/s, $k_2 = 4 \times 10^{-5}$ m/s, $n_1 = 0.5$ (1/m) and $n_2 = 1.4$ (1/m). In thick colluvium the bulk density decreases rapidly with depth and by about 1.5 m the saturated conductivity is not distinguishable from that of the bedrock. Hence we set h_0 equal to 1.5 m. There is considerable uncertainty about these parameters and we explore the effects of different parameter values.

Figure 7 shows the predicted and observed pattern of slope instability for the strength and hydrological parameters estimated above (values given in the figure legend). A logarithmic scale of q/k_1 is used to show the full range of possible values. All but 3 of the 43 scars fall within the instability zones with 80% at least partly touch an area within $\log(q/k_1)$ of less than −2.5, i.e. $q/k_1 = 0.00316$. For this instance in which we estimate $k_1 = 2 \times 10^{-4}$ m/s, the steady-state daily rainfall corresponding to $\log(q/k_1)$ of −3.1, −2.8, −2.5, −2.2 and −1.9 is 1.4, 2.7, 5.5, 10.9 and 21.8 cm/d, respectively. Note that if this estimate of k_1 is roughly correct, an extremely high steady-state rainfall is necessary to cause instability of the steep side slope and ridges.

Figure 8 shows a map of the relative amount of rainfall necessary to cause instability for four values of cohesion: zero, 1000, 5000 and 13 000 N/m². These values represent no vegetation, grass, brush and hardwood trees, respectively (e.g. Reneau and Dietrich, 1987a). This shows how root cohesion strongly affects the range of topographic settings where instability is likely to occur and the intensity of rainfall needed to cause instability. With decreasing root strength, areas of predicted instability spread up to the valleys and onto the ridges. The importance of root cohesion is not a new finding, but these maps appear to be the first portrayal of how realistic changes in root strength with vegetation type alters the location and relative instability of the land.

The four maps in Figure 8 may represent the effects of land-use and climate change. The highest root cohesion (13 000 N/m²) would be associated with forest that might have covered this area during glacial period. The warmer, drier climate of the interglacials resulted in brush and grasslands (5000 N/m²). Grazing and fire could reduce the root cohesion to chronically low values of 1000 N/m² and locally to values of zero.

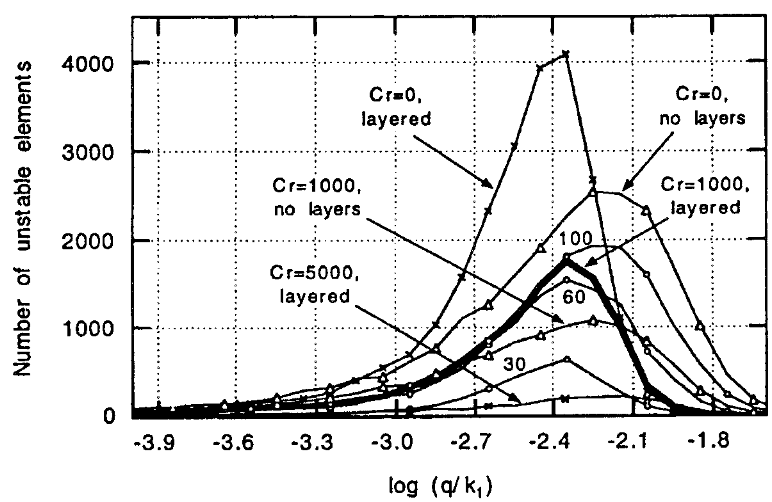

Figure 9. Number of elements that are predicted to have shallow landslides as a function of the logarithm of the net precipitation divided by the surface saturated conductivity for varying strength, soil depth and hydrological properties. The bold black line is the example shown in Figure 7. The two lines labelled with x's are the zero and 5000 N/m² cohesion example shown in Figure 8. The three lines labelled with circles show the instability distribution for constant soil depths of 30, 60 and 100 cm, but otherwise the same parameters as the case represented by the bold black line. The two lines labelled with triangles show the effect of having no contrast (no layers) between the soil and bedrock conductivities — that is, there is a single exponential decline in conductivity from the ground surface to infinity, for the case of $C_r = 0$ and for $C_r = 1000$ N/m².

Given the uncertainty about the parameters in Equation (16), we have performed a number of sensitivity analyses. Figure 9 summarizes some of our findings. This shows the number of elements that are unstable for a given value of $\log(q/k_1)$, with the heavy line being the example shown in Figure 7. Three findings are apparent in this figure. Firstly, if the soil is more conductive and varies less in its conductivity with depth than the underlying bedrock, then less precipitation is required to cause instability and the area of instability is much greater. Compare '$C_r = 0$, layered' with '$C_r = 0$, no layers', the latter being the case in which the saturated conductivity declines uniformly with depth across the soil–bedrock boundary and there is significant flow in the bedrock. The bold line and the line labelled '$C_r = 1000$, no layers' and marked with triangles is this same comparison for $C_r = 1000\,\mathrm{N/m^2}$. If there is no variation with depth ($k_1 = k_2$, $n_1 = n_2$) and n_1 is small ($n_1 < 2$), then deep flow in the bedrock occurs and instability is focused on the unchannelled valleys.

Secondly, soil depth has a large effect on the pattern of relative slope stability. Shallow soils (30 cm) are held in place even with minor root cohesion ($1000\,\mathrm{N/m^2}$) and few elements are unstable. With increasing thickness, the areas of predicted instability spread up the ridges. Uncertainty in an appropriate mean soil depth has a large effect on the pattern of predicted instability. The soil depth model, on the other hand, systematically and correctly predicts thin soils on the ridges and thick in the valleys, which has the effect when combined with the influence of root cohesion of making ridges more stable because of the larger influence of root strength. There are relatively small differences between the model for a constant soil depth of 60 cm and the predicted spatially variable soil depth, although again we found that the instability is spread further up the ridges with the constant soil depth. In a practical application it would be difficult to claim that the slope instability based on the spatially variable soil depth and that based on a 60 cm soil depth are different. The challenge would be to estimate a representative average depth. If part of the hazard is defined by the potential volume that can be released, however, then the spatially uniform soil depth model is inferior because it will either underestimate by large amounts the volume in unchannelled valleys or it will greatly overestimate the side slope and ridge instability (by predicting too great a soil depth there).

Finally, Figures 8 and 9 clearly show the effect of varying root cohesion on relative stability. Much more than any other parameter, root strength can rapidly change due to local effects such as disease and due to large-scale effects such as land-use, fire or climate change.

DISCUSSION

We have attempted to formulate the soil depth and slope stability models on a physical basis with a minimum number of parameters and to make these parameters quantifiable from field observations or mechanical analysis. In the soil depth model, the diffusion coefficient can be estimated by a variety of field methods, as described in this paper. The soil production law has not previously been quantified, and here it is only very crudely estimated as an exponential function of soil depth. The soil production law subsumes all weathering processes inside the production function, ignoring chemical losses that occur during soil transport. No effects of velocity structure with depth are considered. If soil transport is by a linear slope-dependent processes, then our model suggests that because local equilibrium is quickly established, field measurements of soil depth and local curvature would define the shape of the soil production function [see Equation (5)]. A field study is underway to test this hypothesis.

The extent of bedrock exposure also places an important constraint on the production function and diffusivity. According to Equation (6), bedrock will crop out wherever

$$\nabla^2 z > \frac{1}{K}\frac{\rho_r}{\rho_s}\frac{\partial e}{\partial t}$$

that is, where the topographic curvature exceeds the production rate divided by the diffusivity. If the digital elevation data are of sufficiently high resolution to define the local curvature in areas of bedrock exposure, then this criteria can be used to set this ratio, and if the diffusivity can be estimated, then the maximum production rate can be determined.

Spatial variability in diffusion and production, however, is difficult to quantify. These rates probably vary with rock type, climate and the soil biota. Large differences in diffusion coefficient have been identified with rock type (e.g. McKean *et al.*, 1993), but climatic dependency is not well established (see review in Fernandes and Dietrich, in prep.).

If the results of the soil depth model are viewed from the perspective of a longer term landscape evolution, important questions are also raised. Figure 3 shows that the soil depth on ridges is predicted to vary widely across the landscape. Local equilibrium is established between production and erosion and production varies exponentially with depth. This implies that there is a large variation in rates of erosion and the land is far from morphological dynamic equilibrium — even though the soil depth is locally in equilibrium. Only when the ridges have a contact curvature, $\nabla^2 z$, will the erosion rate by diffusive transport be spatially uniform, hence the mapping of curvature from high-resolution digital data may prove a useful method to examine landscape equilibrium tendencies. Spatial variation in diffusivity, K, although certainly likely, would have to covary with curvature for the ridges at our study site to be eroding at a constant rate. This seems unlikely. Bedrock outcrops in a soil-mantled landscape may also indicate a non-steady-state landscape, because bedrock crops out either at locations of maximum erosion (exponential production law) or minimum erosion (maximum production at some finite depth). Changes in diffusivity or production rate with time could change the extent of bedrock outcrop and the spatial dependency of depth or curvature, but unless the model is incorrect, non-uniform curvature values for ridges imply a spatially variable erosion rate.

All the strength and hydrological parameters in the slope stability model can be obtained from field measurements or laboratory analysis. In practice, however, some of these parameters are difficult to define, particularly with regard to their spatial variation. Even for our small study area, we have extrapolated parameters from nearby areas and assumed no spatial variation in their magnitudes.

Our hydrological model for the case in which $k_1 = k_2$, $n_1 = n_2$ of Equation (14) is similar to that used in TOPMODEL (Beven and Kirkby, 1979), which can be written as

$$qa = km \tan\theta e^{-y/m} \tag{18}$$

in which, to convert to our model, $m = -1/n$, $y = y_w \cos\theta$ and $a = a/b$. Note, however, that we use the more physically correct $\sin\theta$ rather than $\tan\theta$, which is important on steep slopes. Also, Equation (14) allows us to examine, explicitly, the effect of conductivity contrasts between bedrock and soil. Our k values reported here are low for catchment scale applications of TOPMODEL (M. J. Kirkby, pers. comm.). Our estimates are based on field measurements and we suggest that the lower values may be more appropriate for hillslopes rather than entire catchments. Also, our n values are very high compared with those used in TOPMODEL (M. J. Kirkby, pers. comm.). Again, this may be a scale effect in that our estimates of n come from field measurements of conductivity on hillslopes and are used to predict only local hillslope response, not catchment scale runoff.

The study by Okimura (1989) offers an instructive comparison with our resuilts. Guided by earlier modelling work using digital elevation data and a coupled slope stability and hydrological model which solves for the pore pressure necessary to cause instability as a function of time since the start of rainfall (Okimura and Kawatani, 1987), Okimura conducted a field study to document the spatial variation in potential failure layer thickness. This layer is identified on the basis of cone penetration results and therefore may not correspond to our definition of soil. Unlike our field observations on soil thickness and our modelling results, he found no systematic relationship with topography and attributed this to effects of past failures. Similar to our findings, however, he concluded that using the measured or estimated spatial distribution of potential failure depth gave very different results from assuming a model with a spatially constant estimated mean depth. He also showed that the number of elements classified as unstable increases significantly with increasing mean depth. Okimura's model does not consider the effects of exponential decline in conductivity with depth, nor the effects of flow in bedrock.

Despite the general success of models based on the infinite slope assumptions, hillslope failures in detail are not necessarily well represented by the infinite slope model, especially when root cohesion matters (e.g. Burroughs *et al.*, 1985). For example, the size of landslides varies with root strength and, therefore, vegetation (e.g. Reneau and Dietrich, 1987a). Also, field observations at sites of shallow failure often suggest that instability was initiated by erosion of the toe due to channel head advance. Local exfiltration gradients associated with bedrock fracture heterogeneity may be responsible for the timing and location of landslides (e.g. Wilson and Dietrich, 1987; Montgomery *et al.*, 1990). These local effects are not included in the infinite slope model and may be more important than the uncertainty in some of the model parameters.

Is the more complicated slope stability model proposed here a substantial improvement over our earlier, two-parameter model that does not include effects of soil depth variation, vertically varying conductivity or root strength? In terms of gaining insight regarding controls or slope stability, we suggest the answer is 'yes'. But with regard to the practical application to slope stability, the answer is less certain. Analysis by Montgomery and Dietrich (1994) of the same study site using our earlier simpler model yielded equally successful results in identifying failure sites. This is partly due to the low root cohesion in this area. When the root cohesion is large, the more complicated model will predict a much smaller area of potential instability than the earlier simpler model. The simpler model cannot be used to ask questions about effects of vegetation changes or differences in bedrock or soils (as influencing vertically varying conductivities). Field studies may eventually yield ranges of diffusivities and soil production laws and their environmental controls such that the soil model will be fairly easy to apply to a new area in a manner that correctly portrays the gross spatial variation in soil depth. Unfortunately, for essentially all practical purposes, the hydrological component of the slope stability model cannot be calibrated, as details of the subsurface conductivity field are rarely known and are not easily obtained.

The large influence of cohesion on the spatial extent of instability (Figures 8 and 9) presents a specific dilemma. Root cohesion is the most variable of all of the slope stability parameters. Fire, disease, land-use, the effects of extreme weather events may all cause local or watershed-wide rapid changes in root strength. How should a map of slope stability with a specific root cohesion be interpreted? For example, consider a long, weakly convergent 30° hillslope with dense vegetation on it which, due to root strength, is estimated to be stable even when saturated. Is it safe to build a house downslope? Is this a site that does not experience landsliding? Our geomorphic analysis might clearly say 'no', as the weakly convergent topography may be a partially infilled bedrock hollow where periodic landslides occur. Presumably the most cautious approach is to assume that at some time the root cohesion can be reduced to zero. There is a lot of land, however, between the area predicted to be unstable with no cohesion and that with a modest amount of cohesive strength which may have considerable value.

Further work is needed on how to incorporate the importance of root strength into land-use decisions. If the conservative approach of assuming no root strength is used (which can be done with the two-parameter model), then vast areas of land in steep hilly areas would be considered potentially unstable — and that is probably correct on geomorphic time-scales, but may be less easily defended on a management time-scale. An approach that has been explored is to treat root strength and other parameters probabilistically (e.g. Hammond *et al.*, 1992) or, in the case of timber harvest, a function of time since cutting (e.g. Sidle, 1992). Although the assignment of probability functions remains largely guesswork, an approach of this kind seems warranted in the context of land-use decisions.

Unlike rivers, which progressively drain larger areas with increasing total catchment area, hillslopes are of only local extent, even in large watersheds. Soil depth and shallow slope instability are strongly dictated by local topography. Therefore, it is desirable to retain the local physical basis of these models when applying them to large watersheds. The simplicity of these models allows this, although again it may be necessary to assume that parameters do not vary significantly over local scales. Hence, although it is desirable and probably necessary to develop ways of representing the hydrological response of large areas by means other than the summing up of all the detailed processes, for soil depth and slope stability analysis the limited spatial extent of hillslopes and the importance of local processes argues for retaining the fine scale analysis. If the goal is to model sediment flux, then perhaps the diffusivity, like saturated conductivity, can be treated as a scale-dependent parameter (e.g. Koons, 1989). A field calibrated transport law for soil flux from shallow landsliding is not available, hence analysis of scaling issues for this process seems premature.

CONCLUSIONS

The simple model for soil depth proposed here appears to explain the general tendency in hilly landscapes for the sharp convex ridges to have thin soil or bedrock outcrop and the swales or unchannelled valleys to be mantled with thick soils. The model also sheds some light on the likely form of a 'law' for the rate of conversion of bedrock to soil. Soil depth rapidly develops a locally stable value for a given curvature. There is no stable value for soil depths thinner than that at which maximum production occurs. Because thin soils are common in steep, sharp-crested hillslopes, this suggests that the maximum production rate of soil probably occurs at nearly zero soil depth. The shape of the production function for the case of soil transport by a linear slope-dependent diffusive process is given by the variation of soil depth with local topographic curvature. These model results suggest specific field observations that should lead to an enhanced understanding of soil production rates.

With the ability to predict soil depth, it is possible to use the infinite slope model to analyse the influence of root cohesion and subsurface conductivity structure on the spatial distribution of shallow landslide potential on real landscapes. Root cohesion affects the total area prone to slope instability and the relative amount of precipitation needed to cause landslides. The variation in saturated conductivity with depth partly controls the relative instability of hollows or unchannelled valleys versus steep side slopes. The less conductive the bedrock relative to that of the soil, the less stable the side slopes. Root cohesion increases the stability of side slopes relative to hollows. However, root cohesion, unlike other parameters affecting soil strength, can vary widely in time due to land use, climate or biological processes such as disease. This sensitivity may give it a dominant role in linking land-use and climate change to slope stability.

ACKNOWLEDGEMENTS

This paper benefited greatly from instructive reviews by M. J. Kirkby, A. D. Howard and A. Rinaldo, as well as two anonymous reviewers. M. J. Kirkby, A. D. Howard, L. Band, N. Fernandes and J. Kirchner also provided critical insights through conversations during various phases of the analysis reported here. Ian Moore offered valuable encouragement and is greatly missed. Kent Rich rescued and improved several of the illustrations. The project was supported by grants TFW FY92-010 and TFW FY94-004 through the CMER and SHAMW committees of the Washington State Timber/Fish/Wildlife agreement.

REFERENCES

Ahnert, F. 1970. 'A comparison of theoretical slope models with slopes in the field', *Z. Geomorphol. Suppl Bd*, **9**, 88–101.

Ahnert, F. 1988. 'Modelling landform change' in Anderson, M. G. (Ed.), *Modelling Geomorphological Systems*. Wiley, Chichester. pp. 375–400.

Anderson, R. S. and Humphrey, N. F. 1989. 'Interaction of weathering and transport processes in the evolution of arid landscapes' in Cross, T. A. (Ed.), *Quantitative Dynamic Stratigraphy*. Prentice Hall, Englewood Cliffs. pp. 349–361.

Beven, K. and Kirkby, M. J. 1979. 'A physically based variable contributing area model of basin hydrology', *Hydrol. Sci. Bull.*, **24**, 43–69.

Black, T. A. and Montgomery, D. R. 1991. 'Sediment transport by burrowing mammals, Marin County, California', *Earth Surf. Process Landforms*, **16**, 163–172.

Brimhall, G. H., Chadwick, O. A., Lewis, C. J., Compston, W., Dietrich, W. E., Power, M. E., Hendricks, D., and Bratt, J. 1992. 'Deformational mass transport and invasive processes in soil evolution', *Science*, **255**, 695–702.

Burroughs, E. R. Jr, Hammond, C. J., and Booth, G. D. 1985. 'Relative stability estimation for potential debris avalanche sites using field data' in Takei, A. (Ed.), *Proceedings of the International Symposium on Erosion, Debris Flow and Disaster Prevention*. Erosion Control Society, Tokyo. pp. 335–339.

Carson, M. A. and Kirkby, M. J. 1972. *Hillslope Form and Process*. Cambridge University Press, Cambridge. 475pp.

Costa, J. E. and Wieczorek, G. F. 1987. 'Debris flows/avalanches: process, recognition and mitigation', *Geol. Soc. Am. Rev. Engin. Geol.*, Vol. VII. Geological Society of America, Boulder. 239pp.

Cox, N. J. 1980. 'On the relationship between bedrock lowering and regolith thickness', *Earth Surf. Process.*, **5**, 271–274.

Crozier, M. J., Vaughn, E. E., and Tippett, J. M. 1990. 'Relative instability of colluvium-filled bedrock depressions', *Earth Sur. Process Landforms*, **15**, 329–339.

Culling, W. E. H. 1963. 'Soil creep and the development of hillside slopes', *J. Geol.*, **71**, 127–161.

Davis, W. M. 1892. 'The convex profile of badland divides', *Science*, **20**, 245.

DeRose, R. C., Trustrum, N. A., and Blaschke, P. M. 1991. 'Geomorphic change implied by regolith–slope relationships on steepland hillslopes, Taranaki, New Zealand', *Catena*, **18**, 489–514.

DeRose, R. C., Trustrum, N. A., and Blaschke, P. M. 1993. 'Post-deforestation soil loss from steepland hillslopes in Taranaki, New Zealand', *Earth Surf. Process Landforms*, **18**, 131–144.
Dietrich, W. E. and Dunne, T. 1978. 'Sediment budget for a small catchment in mountainous terrain', *Z. Geomorphol. Suppl. Bd.*, **29**, 191–206.
Dietrich, W. E., Wilson, C. J., and Reneau, S. L. 1986. 'Hollows, colluvium and landslides in soil-mantled landscapes' in Abrahams, A. (Ed.), *Hillslope Processes, Sixteenth Annual Geomorphology Symposium*. Allen and Unwin, London. pp. 361–388.
Dietrich, W. E., Wilson, C. J., Montgomery, D. R., McKean, J. and Bauer, R. 1992. 'Erosion thresholds and land surface morphology', *Geology*, **20**, 675–679.
Dietrich, W. E., Wilson, C. J., Montgomery, D. R. and McKean, J. 1993. 'Analysis of erosion thresholds, channel networks and landscape morphology using a digital terrain model', *J. Geology*, **101**, 161–180.
Gessler, P. E., Moore, I. D., McKenzie, N. J., and Ryan, P. J., Soil–landscape and spatial prediction of soil attributes', *Int. J. GIS*, in press.
Gilbert, G. K. 1877. *Report of the Geology of the Henry Mountains (Utah), US Geographical and Geological Survey of the Rocky Mountains Region*. US Government Printing Office, Washington, DC. 169pp.
Gilbert, G.K. 1909. 'The convexity of hilltops', *J. Geol.*, **17**, 344–350.
Hammond, C., Hall, D., Miller, S., and Swetik, P. 1992. 'Level 1 Stability Analysis (LISA) documentation for Version 2.0, *USDA, Forest Service, Intermountain Research Station, General Tech. rep. INT-285*, 190pp.
Howard, A. D. 1994. 'A detachment-limited model of drainage basin evolution', *Wat. Resour. Res.*, **30**, 2261–2285.
Kirkby, M. J. 1971. 'Hillslope process-response models based on the continuity equation', *Inst. Br. Geogr. Spec Publ.*, **3**, 15–30.
Kirkby, M. J. 1985. 'A model for the evolution of regolith-mantled slopes' in Woldenberg, M. J. (Ed.), *Models in Geomorphology*. Allen and Unwin, London. pp. 213–228.
Koons, P. O. 1989. 'The topographic evolution of collisional mountain belts: a numerical look at the Southern Alps, New Zealand', *Am. J. Sci.*, **289**, 1041–1069.
McKean, J. A., Dietrich, W. E., Finkel, R. C., Southon, J. R., and Caffee, M. W. 1993. 'Quantification of soil production and downslope creep rates from cosmogenic ^{10}Be accumulations on a hillslope profile', *Geology*, **21**, 343–346.
Montgomery, D. R. 1991. 'Channel initiation and landscape evolution', *Unpubl. PhD Dissertation*, University of California, Berkeley, 421pp.
Montgomery, D. R. and Dietrich, W. E. 1989. 'Channel initiation, drainage density and slope', *Wat. Resour. Res.*, **25**, 1907–1918.
Montgomery, D. R. and Dietrich, W. E. 1994. 'A physically based model for topographic control on shallow landsliding', *Wat. Resour. Res.*, **30**, 1153–1171.
Montgomery, D. R. and Dietrich, W. E. 'Hydrologic processes in a low-gradient source area', *Wat. Resour. Res.*, in press.
Montgomery, D. R., Dietrich, W. E., Torres, R., Anderson, S. P., Heffner, J. T., Sullivan, K. O., and Loague, K. M. 1990. 'Hydrologic experiments in a steep unchanneled valley: (1) experimental design and piezometric response', *EOS, Trans. Am. Geophys. Union*, **71**, 1342.
Moore, I. D., Gessler, P. E., Nielsen, G. A. and Peterson, G. A. 1993. 'Soil attribute prediction using terrain analysis', *Soil Sci. Soc. Am. J.*, **57**, 443–452.
Mulder, H. F. H. M. 1991. 'Assessment of landslide hazard', *Doctoral Thesis*, Faculty of Geographical Sciences, University of Utrecht, 150pp.
Okimura, T. 1989. 'Prediction of slope failure using the estimated depth of the potential failure layer', *J. Natural Disaster Sci.*, **11**, 67–89.
Okimura, T. and Kawatani, T. 1987. 'Mapping of the potential surface-failure sites on granite slopes' in Gardiner, V. (Ed.), *International Geomorphology 1986, Part I*. Wiley, Chichester. pp. 121–138.
Reneau, S. L. 1988. 'Depositional and erosional history of hollows: application to landslide location and frequency, long-term erosion rates, and the effects of climatic change', *Unpubl. PhD Dissertation*, University of California, Berkeley, 328 pp.
Reneau, S. L. and Dietrich, W. E. 1987a. 'Size and location of colluvial landslides in a steep forested landscape', *Proc. Int. Symp. Erosion and Sedimentation in the Pacific Rim, 3–7 August 1987, Corvallis, OR, USA, Int. Assoc. Hydrol. Sci. Bull. Publ. No. 165*, 39–48.
Reneau, S. L. and Dietrich, W. E. 1987b. 'The importance of hollows in debris flow studies' in Costa, J. E. and Wiezcorek, G. F. (Eds), *Debris Flows/Avalanches: Process, Recognition and Mitigation, Geol. Soc. Am. Rev. Engin. Geol.* Vol. VII. Geological Society of America, Boulder. pp. 165–180.
Reneau, S. L., Dietrich, W. E., Rubin, M., Donahue, D. J., and Jull, J. T. 1989. 'Analysis of hillslope erosion rates using data colluvial deposits', *J. Geol.*, **97**, 45–63.
Reneau, S. L., Dietrich, W. E., Donahue, D. J., and Jull, A. J. T. 1990. 'Late Quaternary history of colluvial deposition and erosion in hollows, Central California Coast Ranges', *Geol. Soc. Am. Bull.*, **102**, 969–982.
Selby, M. 1993. *Hillslope Materials and Processes*. Oxford University Press, Oxford. 289pp.
Sidle, R. C. 1992. 'A theoretical model of the effects of timber harvesting on slope stability', *Wat. Resour. Res.*, **28**, 1897–1910.
Wilson, C. J. 1988. 'Runoff and pore pressure development in hollows', *Unpubl. PhD Dissertation*, University of California, Berkeley, 284pp.
Wilson, C. J. and Dietrich, W. E. 1987. 'The contribution of bedrock groundwater flow to storm runoff and high pore pressure development in hollows', in *Proc. Int. Symp. on Erosion and Sedimentation in the Pacific Rim, 3–7 August 1987, Corvallis, OR, USA, Int. Assoc. Hydrol. Sci. Bull. Publ. No. 165*, 49–59.
Wilson, C. J., Dietrich, W. E. and Narasimhan, T. N. 1989. 'Predicting high pore pressures and saturation overland flow in unchannelled hillslope valleyes', in *Proc. Hydrol. and Wat. Resour. Symp.* Institute of Engineers Australia. pp. 392–396.
Wu, W. 1993. 'Distributed slope stability analysis in steep, forested basins', *Unpubl. PhD Dissertation*, Utah State University, 134pp.